Electric conductivity and chloride ingress in hardened cement paste

Kiyofumi Kurumisawa, Toyoharu Nawa

Journal of Advanced Concrete Technology, volume 14 (2016), pp. 87-94

Scientific paper

Electrical Conductivity and Chloride Ingress in Hardened Cement Paste

Kiyofumi Kurumisawa[1*] and Toyoharu Nawa[2]

Received 16 October 2015, accepted 3 March 2016 doi:10.3151/jact.14.87

Abstract

The transport properties of hardened cement paste (HCP) have been investigated in many studies; the AC impedance method (ACI) is a non-destructive technique employed for this purpose and has been used in investigations of the electrical characteristic and mass transport properties of HCP. However, there are relatively fewer studies investigating chloride ingress in HCP and using the ACI. In this study, the relationship between the electrical conductivity measured by the ACI and chloride ingress was investigated. Backscattered electron image analysis and mercury intrusion porosimetry and water porosity were used to measure the pore structure of HCP, and the chloride ingress depth was measured by an electron probe microanalyzer. There was a high correlation between the porosity and conductivity and between the conductivity and diffusion coefficient of the chloride ions in HCP. This implies that the diffusion coefficient of chloride ions could be estimated by the conductivity measurements.

1. Introduction

The durability of concrete is strongly influenced by its transport properties, which may be described by its permeability and diffusion characteristics. Therefore, it is very important to be able to predict and control the transport properties of concrete in order to improve its characteristics. To achieve this, a reduction of the water to cement ratio and production of concrete with supplementary materials such as fly ash and blast furnace slag have been attempted. However, testing the diffusion coefficient and water permeability to establish the transport properties of concrete is time consuming. It is known that the transport properties of concrete strongly depend on the pore structure and that the diffusion coefficient is related to the porosity, tortuosity, and pore connectivity. Therefore, numerous methods for measurement of the pore structure have been suggested. The mercury intrusion method is widely used for measuring the pore structure. Backscattered electron image analysis (BEI) has also been performed to evaluate the pore structure at the submicron level in recent years (Scrivener 2004). This technique could measure the quantity of pores in two-dimensional sections of samples, and the quantity measured can be considered similar to that in three dimensions by performing a statistical analysis. However, it is impossible to evaluate the connectivity of the pores by BEI.

To evaluate the connectivity of pores, electrochemical methods such as DC impedance or AC impedance measurements are employed. It is possible to measure the electrical conductivity from the bulk electrical resistance of cementitious materials by AC impedance measurements, and Christensen reported an investigation with this technique based on theory and experiments (Christensen *et al.* 1994). Numerous studies based on this technique were reported, and the effectiveness in measuring these properties of concrete has been shown (McCarter and Brousseau 1990; Keddam *et al.* 1997; Gu 1993; Cabeza *et al.* 2002; Sato and Beaudoin 2011; Scuderi *et al.* 1991). McCarter *et al.* (2000) reported that the electrical conductivity and permeability and the diffusion coefficient of mortar showed a good correlation, which shows the relationship between the electrical conductivity and other properties of cement-based materials. In addition, there have been many studies investigating the correlation between the electrical conductivity and other properties of concrete (Andrade 1993; Streicher and Alexander 1995; Sánchez *et al.* 2011; Ortega *et al.* 2012; Shi *et al.* 1999; Díaz *et al.* 2006; Mercado *et al.* 2012; Buenfeld and Newman 1987; Shane *et al.* 2000; Vedalakshmi *et al.* 2008; Neithalath and Jain 2010; Minagawa *et al.* 2010). However, most studies have investigated limited ranges of water to cement ratios (W/C 0.4–0.6), and the relationship between the porosity and conductivity of mortar or concrete, which includes the effect of the interfacial transition zone (ITZ), was established as shown in **Table 1**. Recently, high-strength concrete and high-performance concrete, which display a smaller effect of ITZ, have been widely utilized (Vivekanandam and Patnaikuni 1997; Chen and Liu 2004). High strength concrete contains a considerable amount of cement matrix, whose performance has a marked influence on the performance of the concrete. Therefore, it is necessary to investigate hardened cement paste as cement matrix where there is no effect of ITZ. However, there are few studies on hardened cement paste with a strong emphasis on the properties of concrete and mortar.

[1]Associate Professor, Division of Sustainable Resources Engineering, Faculty of Engineering, Hokkaido University , Sapporo, Japan. *Corresponding author, *E-mail*: kurumi@eng.hokudai.ac.jp
[2]Professor, Division of Sustainable Resources Engineering, Faculty of Engineering, Hokkaido University , Sapporo, Japan.

Table 1 Previous studies of electrical conductivity and properties of cementitious materials.

		1	2	3	4	5	6	7	8	9	10	11
Water/Binder ratio		0.55	0.4	0.4	0.25	0.45	0.4	0.4	0.4	0.67	0.4	0.4
			0.5	0.5	0.5		0.43	0.6		0.54		0.5
												0.6
Specimen type	Paste				○							○
	Mortar	○	○	○		○		○	○			○
	Concrete		○				○			○	○	○
Cement and binder		OPC	OPC	OPC	OPC	OPC	CEM I	OPC	OPC	OPC	OPC	OPC
		GGBS	Fly ash	GGBS	Fly ash		CEM V	SRPC		Portland pozzolana cement	Fly ash	Fly ash
		metakaolin			Silica			Fly ash			Silica fume	GGBS
		micro-silica						GGBS				
Reference		McCarter 2000	Sánchez 2011	Ortega 2012	Shi 1999	Díaz 2006	Mercado 2012	Buenfeld 1987	Shane 2000	Vedalakshmi 2008	Neithalath 2010	Minagawa 2010

SRPC: sulphate resisting Portland cement
GGBS: blast-furnace slag

In this study, we measured the pore connectivity by the AC impedance method; the pore structure was measured by BEI analysis and mercury intrusion porosimetry (MIP), and the purpose of this study is to clarify the relation between these. In addition, the relation between the electrical conductivity and diffusion coefficient of the chloride ions in hardened cement paste was also established. We evaluated the diffusivity of the chloride ions in hardened cement paste by evaluating the potential for mass transfer with the AC impedance method, which can measure this parameter rapidly by a simple and easy setup.

2. Diffusion and electrical conductivity

The diffusion flux of ion specie in porous media is expressed by the Nernst-Planck equation (Andrade 1993; Díaz *et al.* 2006; Mercado *et al.* 2012; Minagawa *et al.* 2010).

$$J_i = D_e \frac{\partial C_i}{\partial x} + \frac{z_i F}{RT} D_e C_i \frac{\partial \varphi}{\partial x} \tag{1}$$

J_i: the flux of an ion species i, D_e: the effective diffusion coefficient of the ion species, C: the concentration of the ion, z: the valence number of the ion species, R: the gas constant, F: Faraday's constant, T: the temperature, φ: the electrical field, and x: the position of medium. When there is no concentration gradient in the porous medium and the external potential is sufficiently large, equation (1) can be simplified as follows.

$$J_i = \frac{z_i F}{RT} D_e C_i \frac{\partial \varphi}{\partial x} \tag{2}$$

Then, to convert the flux J_i to the current density I, both sides of equation (2) are multiplied by z_iF.

$$I = z_i F J_i = \frac{z_i^2 F^2}{RT} D_e C_i \frac{\partial \varphi}{\partial x} \tag{3}$$

Now, the bulk electrical conductivity σ can be expressed by the following equation.

$$\sigma = \frac{I}{\left(\frac{\partial \varphi}{\partial x}\right)} \tag{4}$$

Substituting I from equation (3) gives the following relation (Andrade 1993).

$$\sigma = D_e \frac{z_i^2 F^2 C_i}{RT} \tag{5}$$

This shows that the electrical conductivity is proportional to the effective diffusion coefficient and the concentration of ions. The effective diffusion coefficient D_e and intrinsic diffusion coefficient D_0 are related as follows.

$$D_e = \frac{\varepsilon}{\tau} S^{-m} D_0 \tag{6}$$

ε: the porosity of porous media, τ: the tortuosity, S: the degree of saturation, m: a constant. This shows that the electrical conductivity is also proportional to the porosity, tortuosity, and saturation.

3. Experimental

3.1 Specimens

Ordinary Portland cement (OPC) produced in Japan as shown **Table 2** was used. Six water/cement ratios (0.3, 0.4, 0.5, 0.6, 0.7, and 0.8) were used to produce a variety of microstructures in the hardened cement pastes. The specimens were cast in 40 × 40 × 40-mm cubic molds for the electrical conductivity measurements, and as 50 mm long, 50 mm diameter cylinders for the chloride diffusion measurements. The specimens were demolded after 24 h (except W/C 0.8) and cured at 20 °C and RH = 98% (to maintain moist conditions) for 1, 3, 7, 28, and 91 d.

Table 2 Physical properties and chemical composition of the cement used here.

Density (kg/m^3)		3160
Blaine surface area (cm^2/g)		3450
Chemical composition (wt%)	SiO_2	20.83
	Al_2O_3	5.59
	Fe_2O_3	2.64
	CaO	64.81
	MgO	1.30
	SO_3	2.02
	TiO_2	0.25
	MnO	0.06
	Na_2O	0.23
	K_2O	0.50
	P_2O_5	0.20
	Cl	0.021

3.2 Backscattered electron image (BEI) measurements

A 5 mm cube was cut from the dried samples of the hardened cement pastes (curing ages: 1, 3, 7, 28, 91 d) and used for the BEI observations. The dried specimens were immersed in epoxy resin in vacuum; after the hardening of the epoxy resin, a specimen surface was polished using SiC paper and smoothed by 0.25 μm diamond paste; a carbon coat was applied to provide electrical conductivity to the specimen surface. The electron microscopy imaging was performed under the following conditions: an acceleration voltage of 15 keV, a working distance of 17 mm, a field size of 200 × 150-μm, and a pixel size of 0.32 μm. The resulting resolution in this study is 0.32 μm, and it was not possible to distinguish pores smaller than 0.32 μm in diameter. The observations were made on 16 fields in each specimen. Unhydrated cement (UH), calcium hydroxide (CH), C-S-H (including fine pores and other hydrates), and pores larger than 0.32 μm (coarse porosity) were distinguished using image analysis software and setting brightness thresholds. The average area fraction of each phase was considered to be the volume fraction (Igarashi *et al.* 2004).

3.3 Electrical conductivity

The specimens for the electrical conductivity measurements had a size of 40 × 40 × 40-mm, and the stainless electrodes (40 × 30 × 0.3-mm) were placed 30 mm apart on the specimen. The effective area of the electrode was 30 × 30-mm; the AC impedance of the specimens was measured in the frequency range of 4 Hz to 5 MHz with an impedance analyzer (HIOKI IM3570), and the applied voltage was 0.1 V. After the measurements, a Nyquist plot was established from the acquired data, and the bulk resistance was determined from the point where the electrode response (straight line) and the arc crossed, as shown in **Fig. 1**.

$$\rho = \frac{R_a L}{A} \tag{7}$$

$$\sigma = \frac{1}{\rho} \tag{8}$$

ρ: the bulk resistivity of the specimen, R_a: the measured resistance, L: the distance between electrodes, A: the effective area of the electrode, and σ: the conductivity. It can be seen that the frequency of the measured resistance changed in each specimen. The electrical conductivity of hardened cement paste depends on the porosity, pore connectivity, and conductivity of the pore solution in the hardened cement paste. The result is the normalized conductivity with the influence of the conductivity of the pore solution removed. The conductivity of the pore solution was calculated based on previous studies from the degree of hydration of cement and the chemical composition of the cement (Taylor 1987; Snyder *et al.* 2003).

3.4 Chloride ingress depth measurement

We measured the ingress depth of the chloride ions by an electron probe microanalyzer (EPMA: JEOL JXA-8900M). The specimens were cylindrical (50 mm long, 50 mm diameter cylinders) with curing ages 28 and 91 d, immersed in NaCl 0.5 mol/l solution for 3 weeks; thereafter, the distribution of the elements (Ca, Si, and Cl) was determined by EPMA, and the ingress depth of chloride was established. The apparent diffusion coefficient was determined by the following equation, with the concentration $C(x,t)$ derived from Fick's second law (initial and boundary conditions: $C = C_0$ at $x = 0$, $t > 0$; $C = 0$ at $x > 0$, $t = 0$; $C = 0$ at $x = \infty$, $t = 0$).

$$C(x,t) = C_0 \cdot \left[1 - erf\left(\frac{x}{2\sqrt{D_a \cdot t}}\right)\right] \tag{9}$$

erf: an error function, x: the distance from the exposed face, t: the exposure time, C_0: the bulk concentration, and D_a: the apparent diffusion coefficient.

3.5 Water porosity, mercury intrusion porosimetry and loss of ignition

The water porosity of the specimens was determined from the weights before and after drying at 105 °C and the volume of the specimens. Mercury intrusion porosimetry (MIP) was used to measure the pore size dis-

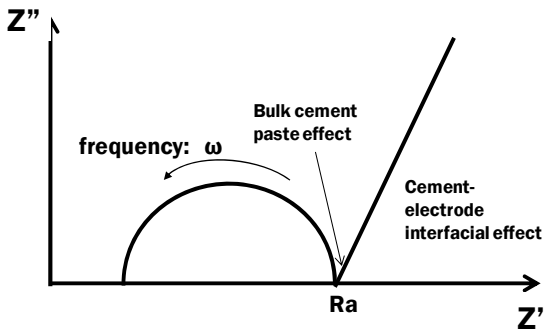

Fig. 1 Nyquist plot of hardened cement paste.

tribution from 6 nm to 100μm diameter in the specimens (curing ages: 3, 28, and 91 d).

The loss on ignition (LOI) from 105 to 950 °C was measured to determine the degree of hydration in the specimens. The degree of hydration of the cement (α) in the ordinary Portland pastes is calculated by equation (10).

$$\alpha = \frac{LOI}{0.23} \tag{10}$$

The denominator (0.23) is the non-evaporable water of fully hydrated cement paste.

4. Results and discussion

4.1 BEI analysis

The BEI observations are shown in **Fig. 2**; the black, dark grey, light grey, and white pixels show pores, C-S-H, CH, and UH, respectively. As the water to cement ratio increases, there are more capillary pores, showing that the specimens with higher water to cement ratios have a more porous structure. The results show that it is possible to produce hardened cement pastes with different microstructures. The area fractions of each phase calculated from the BEI are shown in **Fig. 3**, showing an average of more than 16 BEI images for each specimen. The porosity and unhydrated cement (UH) decreased with the progress of the curing of the specimens at all water to cement ratios, and calcium hydroxide (CH) and C-S-H (including the fine pores of less than 0.32 μm and other hydrates such as monosulfoaluminate or ettringite) increased. The relation between the degree of hydration, calculated from the loss on ignition (LOI), and the quantity of unhydrated cement determined by BEI is shown in **Fig. 4**. The two quantities had a strong positive correlation (≈ 1), establishing that the BEI analysis is able to detect the microstructure of specimens as reported previously (Igarashi 2004; Scrivener 2004).

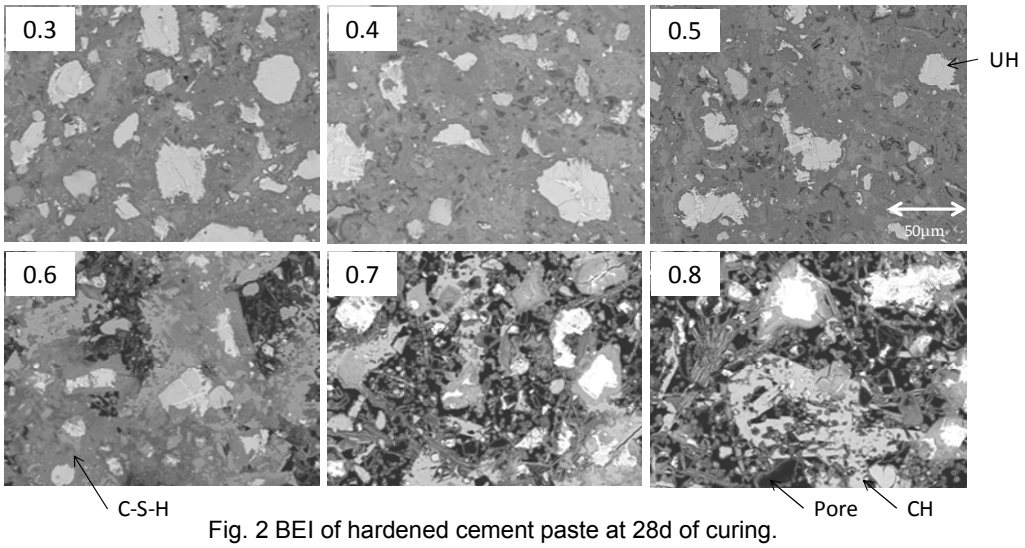

Fig. 2 BEI of hardened cement paste at 28d of curing.

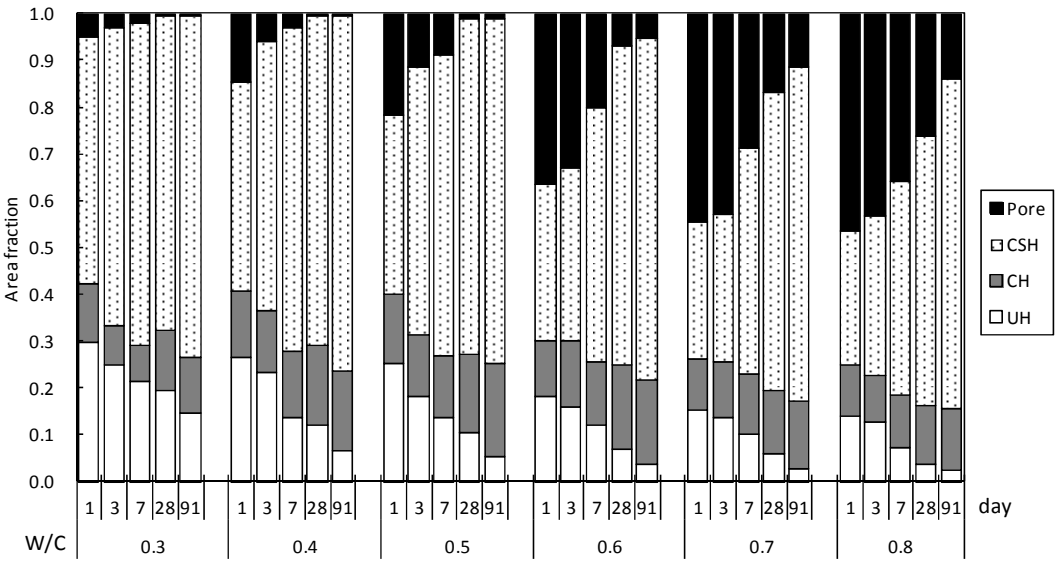

Fig. 3 Area fraction of hardened cement pastes measured by BEI.

4.2 The electrical conductivity

The results of electrical conductivity measurements of the hardened cement pastes with various water to cement ratios are shown in **Fig. 5**. The electrical conductivity of the specimens decreased with decreasing water to cement ratios, and the conductivity of all specimens became very similar after 7 d of curing. This is because porosity measured by BEI as shown in **Fig. 3** greatly decreases until the end of 7 d of curing, but the decrease in porosity is slow after 7 d.

4.3 Chloride ingress and electrical conductivity

The conductivity is dependent on the pore solution conductivity and pore structure parameters such as porosity and tortuosity. The pore solution conductivity is calculated by the methods of Taylor (1987) and Snyder *et al.* (2003) as described in Sec. 3.3, and the normalized conductivity σ_n is established by the following equation.

$$\sigma_n = \frac{\sigma}{\sigma_0} \tag{11}$$

σ is the conductivity, and σ_0 is the pore solution conductivity. The relationship between conductivity and apparent diffusion coefficient of chloride ions at 3 weeks immersion is shown in **Fig. 6**. There is a very strong correlation between the conductivity and the diffusion coefficient of chloride ions in all of the specimens. This result corresponds to the results of the concrete and mortar relationship between conductivity and diffusion coefficients in previous reports (Vedalakshmi *et al.* 2008; Neithalath and Jain 2010; Minagawa *et al.* 2010). Further, the correlation of the normalized conductivity was higher than that of the conductivity; this is because diffusion of chloride ion in hardened cement paste is strongly related to the pore structure. However, both the pore structure of the hardened cement paste and the composition of the pore solution influence the chloride ingress, as shown in equation (6). The effective diffusion coefficient has been shown to be associated with the apparent diffusion coefficient in other experiments (Yang 2005; Chiang and Yang 2007). In summary, it may be concluded that it is possible to predict the chloride ingress by measurement of the electrical conductivity from these relations, and it is also possible to predict the durability of a new concrete structure and evaluate the durability of existing concrete structures. However, it is necessary to consider the effect of the composition of the pore solution and water content in the concrete when the conductivity measurements are applied to evaluate the performance of in situ concrete structures as shown in previous studies (Shi 2004; Saleem *et al.* 1996; Rajabipour and Weiss 2007).

4.4 The electrical conductivity and pore structure

The effect of pore structure on the conductivity was also investigated. Archie reported that the pore structure and normalized conductivity are related by the following equation (Archie 1972):

$$\sigma_n = \varepsilon^m \tag{12}$$

ε is the porosity, and m is the cementation exponent. According to Archie, the value of m lies between 1.8 and

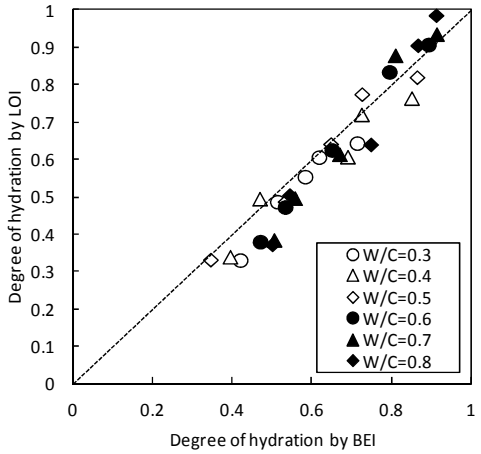

Fig. 4 Plot of degree of hydration measured by BEI and LOI.

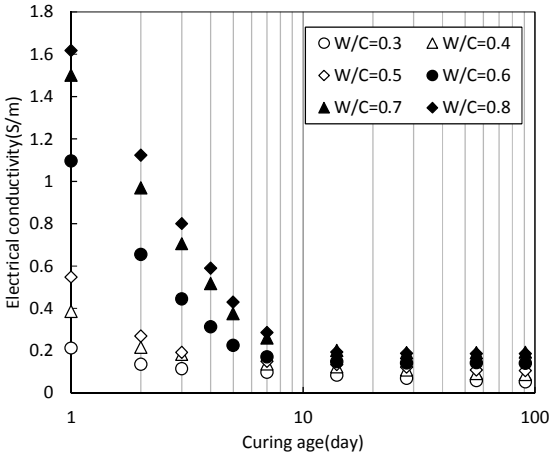

Fig. 5 Change in electrical conductivity of hardened cement pastes with age.

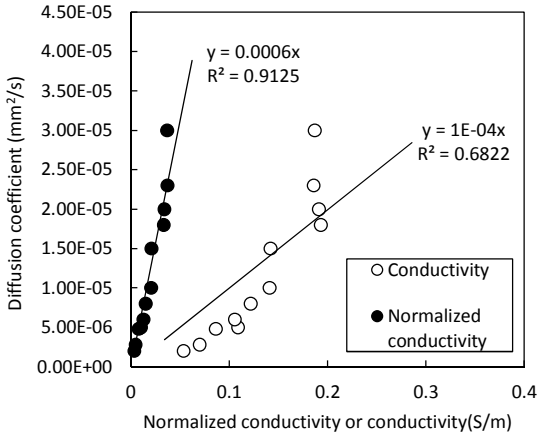

Fig. 6 Plot of conductivity and apparent diffusion coefficient of chloride ions.

2.0 for consolidated sandstone (Archie 1972). As the cementation exponent *m* increases, the complexity of the pore structure increases. The influence of the surface electrical conductivity on the bulk electrical conductivity was not considered in this study, since it was reported by Rajabipour that this effect is 5% or less in the case of saturated hardened cement paste (Rajabipour and Weiss 2007).

The effects of the porosity measured by BEI, the porosity measured by MIP, and the water porosity on the normalized conductivity of hardened cement pastes are shown in **Fig. 7**, **Fig. 8**, and **Fig .9**, respectively. In all specimens, the normalized conductivity decreases with a reduction in the coarse porosity (>0.32 μm) determined by BEI, by the MIP porosity, and by the water porosity. The relation between the porosity and normalized conductivity was determined by exponential functions following Archie's law with equation (12) for all the water to cement ratios and curing ages investigated here. This effectively shows that the complexity of the pore structure of hardened cement paste is very similar at similar porosities. In other words, for similar porosities of hardened cement paste, the connectivity of pores is also similar, even if the water to cement ratio or curing age of the hardened cement paste is different.

The correlation is the highest between the normalized conductivity and porosity measured by MIP as shown in **Fig. 8**. This shows that pores more than 6 nm in diameter influence the electrical conductivity. The normalized conductivity becomes almost zero when the water porosity is below 0.2. Based on the percolation theory, the critical porosity of percolation in three dimensions is around 0.2 and in two dimensions is around 0.5 (Stauffer and Aharony 1992). This shows that it is possible to explain the conductivity in hardened cement paste by percolation theory.

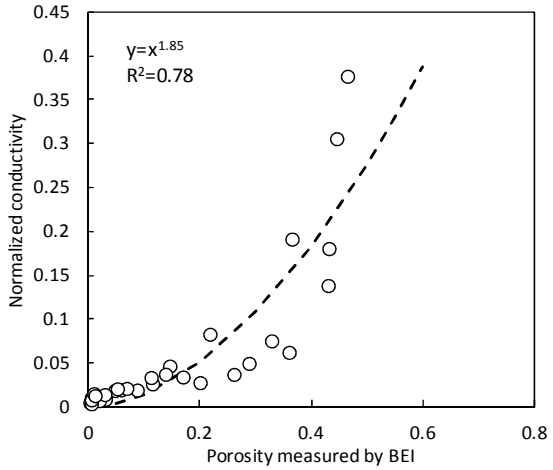

Fig. 7 Effect of porosity measured by BEI on the normalized conductivity.

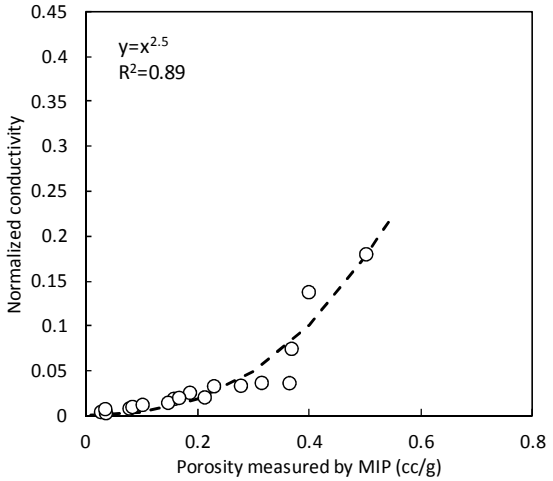

Fig. 8 Effect of porosity measured by MIP on the normalized conductivity.

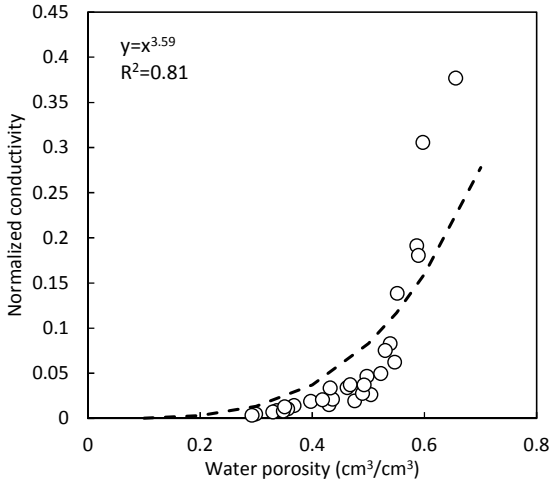

Fig. 9 Effect of water porosity on the normalized conductivity.

5. Conclusions

The electrical conductivity and microstructure of hardened cement paste over a range of water to cement ratios was investigated in this study. The electrical conductivity of hardened cement pastes depends on the porosity measured by MIP as well as on the porosity of large capillary pores that can be detected by backscattered electron images. However, the correlation is the highest between the normalized conductivity and porosity more than 6 nm measured by MIP. These relations can be expressed by Archie's law in all specimens regardless of the water to cement ratio or curing age. Finally, relations between the electrical conductivity and diffusion coefficient of chloride ions in hardened cement paste were established, and it was shown that it is possible to predict the chloride ingress by measurements of the electrical conductivity.

Acknowledgment

We thank the Ministry of Education, Culture, Sports, Science and Technology for financial support with the research here (No. 25420565). And a part of this work was conducted at "Joint-use Facilities: Laboratory of

Nano-Micro Material Analysis", Hokkaido University, supported by "Nanotechnology Platform" Program of the Ministry of Education, Culture, Sports, Science and Technology (MEXT), Japan.

References

Andrade, C., (1993). "Calculation of chloride diffusion coefficients in concrete from ionic migration measurements." Cem. Concr. Res. 23(3), 724-742.

Archie, G. E., (1972). "The electrical resistivity log as an aid in determining some reservoir characteristics." Trans. AIME, 146, 54-62.

Buenfeld, N. and Newman, J., (1987). "Examination of three methods for studying ion diffusion in cement pastes, mortars and concrete." Mater. Struct., 20(1), 3-10.

Cabeza, M., Merino, P., Miranda, A., Nóvoa, X. R. and Sanchez, I., (2002). "Impedance spectroscopy study of hardened Portland cement paste." Cem. Concr. Res., 32(6), 881-891.

Chen, B. and Liu, J., (2004). "Effect of aggregate on the fracture behavior of high strength concrete." Constr. Build. Mater., 18(8), 585-590.

Chiang, C. T. and Yang, C. C., (2007). "Relation between the diffusion characteristic of concrete from salt ponding test and accelerated chloride migration test." Mater. Chem. Phys., 106, 240-246.

Christensen, B. J., Coverdale, T., Olson, R. A., Ford, S. J., Garboczi, E. J., Jennings, H. M. and Mason T. O., (1994). "Impedance spectroscopy of hydrating cement-based materials: Measurement, interpretation, and application." J. Am. Ceram. Soc., 77, 2789-2804.

Díaz, B., Nóvoa, X. R. and Pérez, M. C., (2006). "Study of the chloride diffusion in mortar: A new method of determining diffusion coefficients based on impedance measurements." Cem. Conc. Comp., 28(3), 237-245.

Gu, P., Xie, P. Beaudoin, J. J. and Brousseau, R., (1993). "A.C. impedance spectroscopy (II): Microstructural characterization of hydrating cement-silica fume systems." Cem. Concr. Res., 23(1), 157-168.

Igarashi, S., Kawamura, M. and Watanabe, A., (2004). "Analysis of cement pastes and mortars by a combination of backscatter-based SEM image analysis and calculations based on the Powers model." Cem. Concr. Comp., 26, 977-985.

Keddam, M., Takenouti, H., Nóvoa, X. R., Andrade, C. and Alonso, C., (1997). "Impedance measurements on cement paste." Cem. Concr. Res., 27(8), 1191-1201.

Lu, X., (1997). "Application of the Nernst-Einstein equation to concrete." Cem. Concr. Res., 27(2), 293-302.

McCarter, W. J. and Brousseau, R., (1990). "The A.C. response of hardened cement paste." Cem. Concr. Res., 20(6), 891-900.

McCarter, W. J., Starrs, G. and Chrisp, T. M., (2000). "Electric conductivity, diffusion, and permeability of Portland cement-based mortars." Cem. Concr. Res., 30(9), 1395-1400.

Mercado, H., Lorente, S. and Bourbon, X., (2012). "Chloride diffusion coefficient: A comparison between impedance spectroscopy and electrokinetic tests." Cem. Conc. Comp. 34(1), 68-75.

Minagawa, H., Hisada, M., Ehara, A., Saito, Y., Ichikawa, M. and Inoue, H., (2010). "Fundamental study on relationship between electric resistivity and chloride ion diffusivity of concrete." Doboku Gakkai Ronbunshuu E., 66(1), 119-131 (in Japanese).

Neithalath, N. and Jain, J., (2010). "Relating rapid chloride transport parameters of concretes to microstructural features extracted from electric impedance." Cem. Concr. Res., 40(7), 1041-1051.

Ortega, J. M., Sánchez, I. and Climent, M. A., (2012). "Durability related transport properties of OPC and slag cement mortars hardened under different environmental conditions." Constr. Build. Mater., 27(1), 176-183.

Rajabipour, F. and Weiss, J., (2007). "Electrical conductivity of drying cement paste." Mater. Struct. 40(10), 1143-1160.

Sánchez, I., López, M. P., Ortega, J. M. and Climent, M. Á., (2011). "Impedance spectroscopy: An efficient tool to determine the non-steady-state chloride diffusion coefficient in building materials." Mater. Corros., 62(2), 139-145.

Saleem, M., Shameem, M., Hussain, S. E., and Maslehuddin, M., (1996). "Effect of moisture, chloride and sulphate contamination on the electrical resistivity of Portland cement concrete." Const. Build. Mater., 10(3), 209-214.

Sato, T. and Beaudoin, J. J., (2011). "Coupled AC impedance and thermomechanical analysis of freezing phenomena in cement paste." Mater. Struct. 44(2), 405-414.

Scrivener, K. L., (2004). "Backscattered electron imaging of cementitious microstructures: Understanding and quantification." Cem. Conc. Comp., 26, 935-945.

Scrivener, K. L., Füllmann, T., Gallucci, E., Walenta, G. and Bermejo, E., (2004). "Quantitative study of Portland cement hydration by X-ray diffraction/Rietveld analysis and independent methods." Cem. Concr. Res., 34, 1541-1547.

Scuderi, C. A., Mason, T. O., Jennings, H. M., (1991). "Impedance spectra of hydrating cement pastes." J. Mater. Sci., 26(2), 349-353.

Shi, C., (2004). "Effect of mixing proportions of concrete on its electrical conductivity and the rapid chloride permeability test (ASTM C1202 or ASSHTO T277) results." Cem. Concr. Res., 34(3), 537-545.

Shi, M., Chen, Z. and Sun, J., (1999). "Determination of chloride diffusivity in concrete by AC impedance spectroscopy." Cem. Concr. Res., 29(7), 1111-1115.

Shane, J. D., Mason, T. O., Jennings, H. M., Garboczi, E. J. and Bentz, D. P., (2000). "Effect of the interfacial transition zone on the conductivity of Portland cement

mortars." J. Am. Ceram. Soc., 83(5), 1137-1144.

Snyder, K. A., Feng, X., Keen, B. D. and Mason, T. O., (2003). "Estimating the electric conductivity of cement paste pore solutions from OH^-, K^+ and Na^+ concentrations." Cem. Concr. Res., 33(6), 793-798.

Stauffer, D., and Aharony, A., (1992). "*Introduction to percolation theory*." Taylor & Francis, London.

Streicher, P. E. and Alexander, M. G., (1995). "A chloride conduction test for concrete." Cem. Concr. Res., 25(6), 1284-1294.

Taylor, H. F. W., (1987). "A method for predicting alkali ion concentrations in cement pore solutions." Adv. Cem. Res. 1, 5-17.

Vedalakshmi, R., Renugha, R., Bosco, D. E. and Palaniswamy, N., (2008). "Determination of diffusion coefficient of chloride in concrete: an electrochemical impedance spectroscopic approach." Mater. Struct., 41, 1315–1326.

Vivekanandam, K. and Patnaikuni, I., (1997). "Transition zone in high performance concrete during hydration." Cem. Concr. Res., 27(6), 817-823.

Yang, C. C., (2005). "A comparison of transport properties for concrete using ponding test and the accelerated chloride migration test." Mater. Struct., 38, 313-320.